Full-scale experimental testing and finite element analysis of a totally prefabricated counterfort retaining wall system

Maen Farhat, Mohsen Issa, Mustapha Ibrahim, and Momenur Rahman

- The overall structural behavior of a totally prefabricated counterfort retaining wall system was examined experimentally and analytically using nonlinear finite element analysis.
- The anchors succeeded in maintaining serviceability and ultimate strength requirements.
- The totally prefabricated counterfort retaining wall system has proven to be an innovative and effective solution for multiple requirements, such as speed of construction, strength, durability, and safety.

Increasing traffic demands require further expansion of highway and bridge components, including substructure systems. The conventional construction process performed to accommodate such an expansion is generally accompanied by traffic interruptions, lane closures, and prolonged construction times, which lead to higher costs. As a result, several departments of transportation are seeking accelerated construction techniques to reduce the impact of the long construction periods associated with conventional construction methods. Current accelerated construction techniques use precast concrete systems, which provide several economic advantages over conventional cast-in-place concrete construction methods. The use of precast concrete systems for highway and bridge construction can potentially reduce the site preparation procedures, overall construction period, and environmental impact. Moreover, it is credited with promoting work zone safety and reducing the number of injuries caused by exposing workers to active traffic.

Although precast concrete systems provide several economic, social, and environmental advantages, plenty of research is still required to develop precast concrete systems for substructures such as retaining walls and abutments. As a response, a totally prefabricated counterfort retaining wall system was developed as a retaining wall solution for highway applications. The proposed system was developed and optimized[1,2] as a response to growing needs such as speed of construction, strength and durability, minimization of traffic flow interruption, safety, and cost.

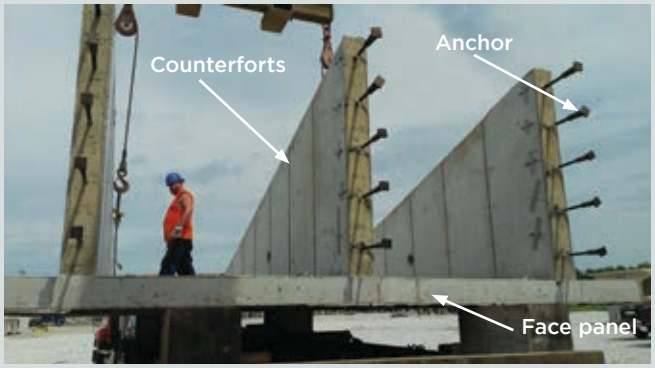

Figure 1. Totally prefabricated counterfort retaining wall system during erection showing anchors extending from the counterfort.

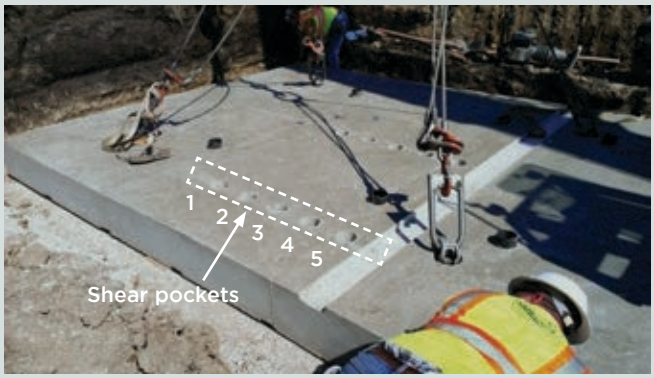

Figure 2. Base slab during erection showing predesigned shear pockets for anchor embedment.

The totally prefabricated counterfort retaining wall system is composed of two prefabricated components: the wall component, consisting of a face panel with three counterforts, and the base slab component (**Fig. 1** and **2**). Counterforts act as stiffeners to the face panel and connect the wall and the base slab. Headed anchors are used to connect each counterfort to the base slab, thus enforcing the integrity of the system to achieve full composite action.

Counterforts are added along the width of the wall at discrete locations to enhance the serviceability of the face panel and to increase the stiffness of the system without increasing the thickness of the face panel. In fact, counterfort retaining wall systems exhibit lower stress states than their cantilever counterparts. Senthil et al.[3] performed a three-dimensional finite element analysis to study the structural performance of both cantilever- and counterfort-type retaining walls subjected to lateral earth pressure. The study shows that retaining walls with counterforts of 1.2 m (3.9 ft) below the top surface of the face panel exhibit lower stress levels than cantilever retaining walls of the same height.

Figure 3 shows the front elevation of the proposed totally prefabricated counterfort retaining wall system and the extended counterforts.

In this study, the overall structural behavior of a totally prefabricated counterfort retaining wall system was experimentally studied and analytically evaluated using nonlinear finite element analysis. A 20 ft 2 in. (6.09 m) high, 13 ft 10 in. (4.21 m) wide, full-scale totally prefabricated counterfort retaining wall prototype was designed in accordance with the requirements of the American Association of State Highway and Transportation Officials' *AASHTO LRFD Bridge Design Specifications*.[4]

The system was manufactured in a precast concrete plant. Headed anchors were embedded in each counterfort during casting with 1 ft (0.3 m) spacing and sufficient develop-

Background

The use of precast concrete elements for bridge construction and rehabilitation is considered economically efficient because it requires less time for construction.[5] Although cast-in-place concrete abutments, piers, and deck slabs are widely used in bridge applications, their construction sequences and procedures are considered time intensive.[6] Several activities related to cast-in-place concrete procedures have created problems related to time schedules, safety priorities, and the environment. These activities include the following:

- site preparation procedures, such as installing formwork and casting and curing concrete
- traffic detours and lane closures, which cause traffic congestion
- construction work that exposes workers to active traffic
- finishing work that requires skilled workers

Figure 3. Front elevation of the totally prefabricated counterfort retaining wall system with wing walls.

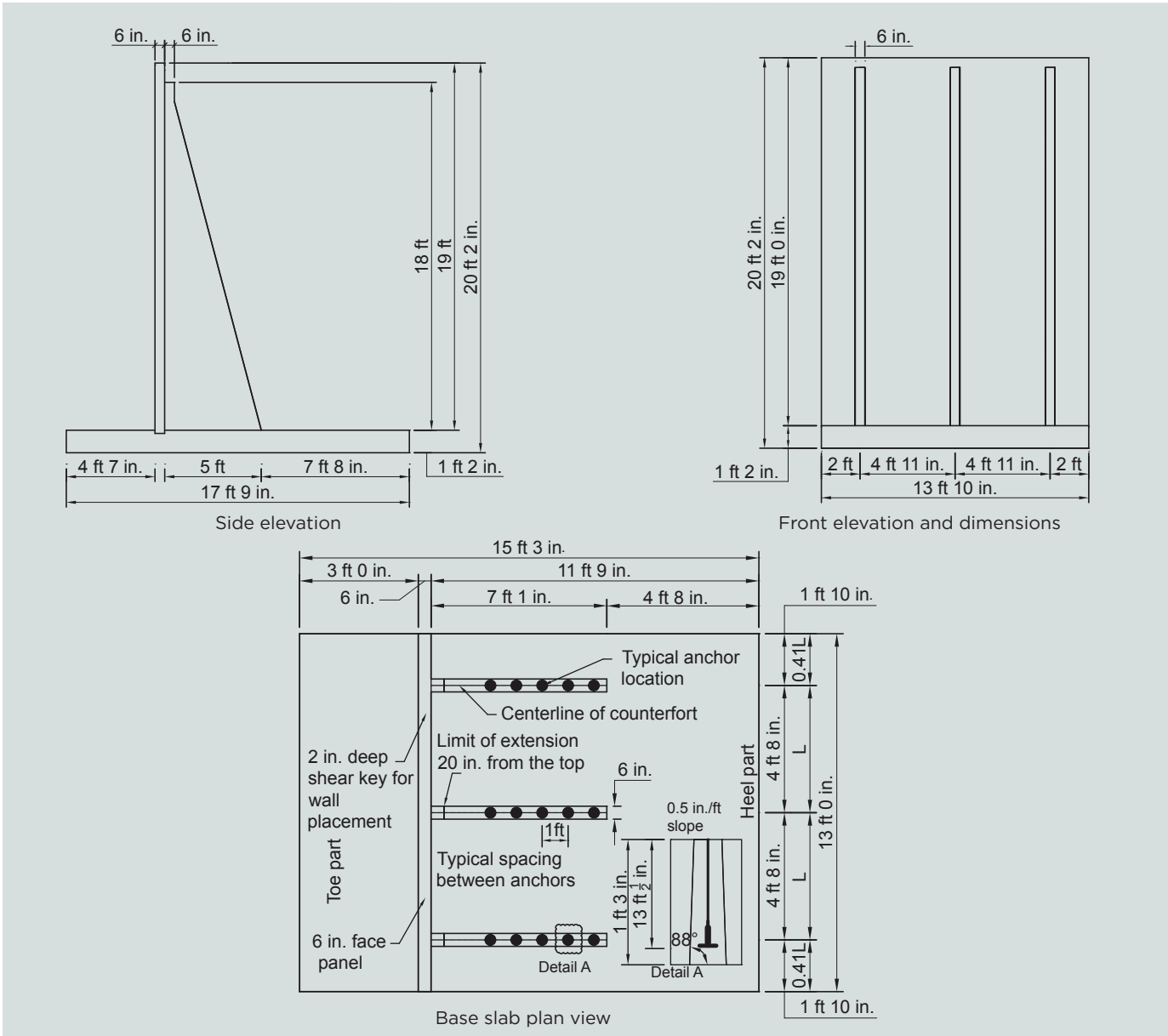

Figure 4. Geometric layouts of the totally prefabricated counterfort retaining wall system. Note: *L* = center-to-center spacing between two adjacent counterforts. 1 in. = 25.4 mm; 1 ft = 0.305 m.

These challenges have led to more focus on precast concrete products due to the efficiency of their production and assembly processes. Moreover, precast concrete products are typically produced in a controlled plant environment, thereby taking advantage of the uniformity and consistency of high-performance concrete properties and reducing the risk of errors on-site.

Precast concrete bridge components are divided into superstructure elements (such as decks and beams) and substructure elements (such as piers, abutments, and retaining walls). Generally, most of the research found in the literature focuses on developing precast concrete superstructure systems.[7–15] The research resulted in details and guidelines for using partially or fully precast concrete superstructure systems.

Numerous studies involve precast concrete bridge components to promote accelerated bridge construction in super- and substructures.[16–21] The use of precast concrete technologies in bridge substructure construction such as bent caps, columns, and footings has been frequently reported;[22–23] however, studies on the development or optimization of the end supports of bridges, such as retaining walls and abutments, are scarce. A precast concrete cantilever retaining wall system was developed by the Michigan Department of Transportation to reduce construction time and improve work zone safety.[24] The precast concrete cantilever-type

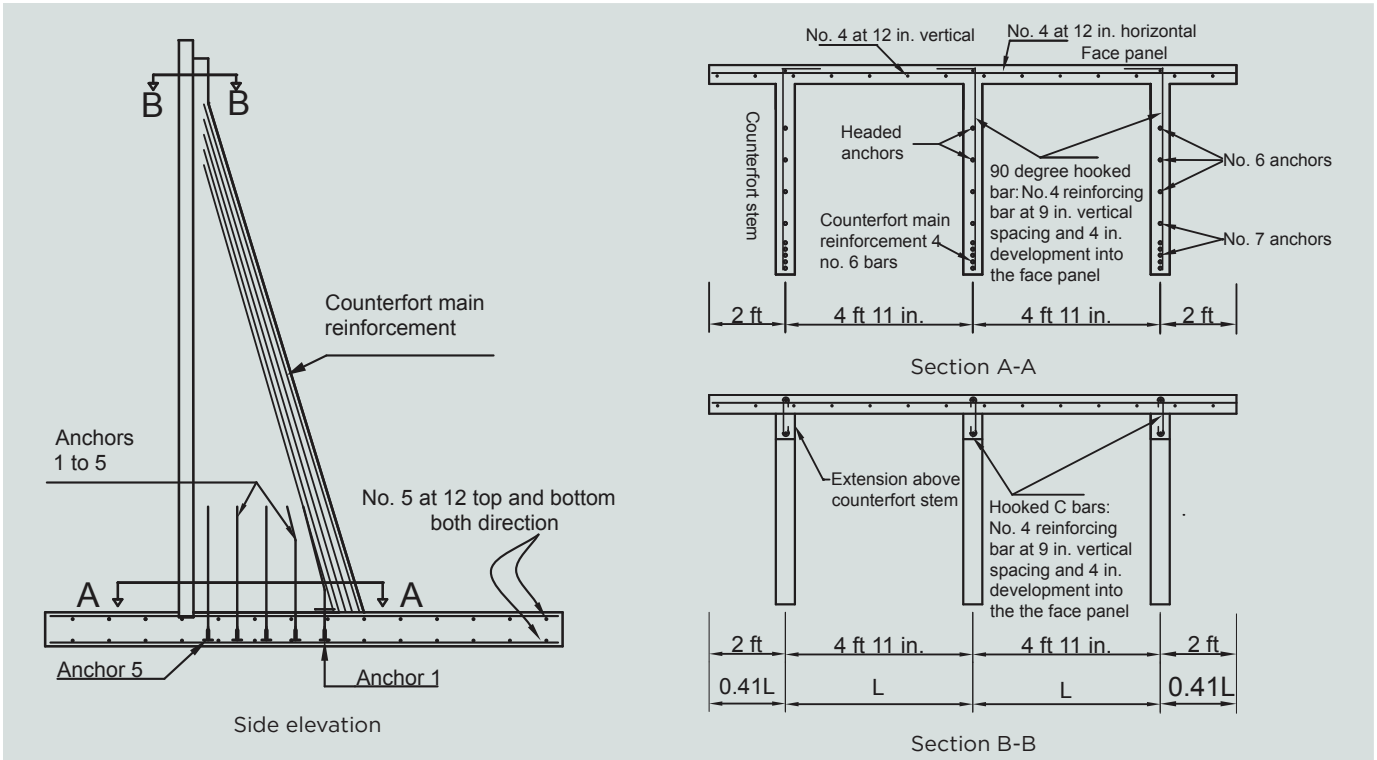

Figure 5. Steel reinforcement details of the totally prefabricated counterfort retaining wall system. Note: *L* = center-to-center spacing between two adjacent counterforts. Note: no. 4 = 13M; no. 5 = 16M; no. 6 = 19M; 1 in. = 25.4 mm; 1 ft = 0.305 m.

walls consisted of 5000 psi (34 MPa) precast concrete footing and stem segments. The height of each segment was limited to 12 ft (3.7 m) to facilitate transportation and erection. Full moment connection was provided between the stem and the footing through grout-filled mechanical splicers. Vertical joints between precast concrete elements used shear keys, which were filled with nonshrink high-strength grout. Retaining wall heights ranged from 4 ft (1.2 m) to a maximum of 26 ft (7.9 m). Because the wall was a regular cantilever wall, a thick wall section was used to control deflection and cracking and meet the structural design considerations.

Similarly, a precast concrete bridge was constructed in only eight days in New Hampshire in 2004.[25] The system consisted of a precast concrete footing and a precast concrete abutment stem. Reinforcement extended from the base footing into predesigned splice sleeve connectors in the precast concrete stem. These sleeves were grouted using high-strength grout through splice ports. The splice sleeves were aligned with the extended bars within a tolerance of ½ in. (13 mm). The wall stem was placed in a pocket to facilitate grouting and improve shear resistance.

In addition, Donkada and Menon[26] have presented an optimization approach with cast-in-place concrete counterfort retaining walls of varying heights that takes into account geometric, reinforcement, and cost parameters. A report summarized the work done in the field and showed details for connections in precast concrete bridge components, including retaining walls and abutments used in various states in the United States.[27]

This study examines the structural performance of the proposed totally prefabricated counterfort retaining wall system through full-scale experimental testing and nonlinear finite element analysis. The structural behavior of each component during load application is presented and compared with the results obtained from the finite element analysis. **Figure 5** summarizes the reinforcement details of the totally prefabricated counterfort retaining wall system. The overall resulting weight of the structure is about 73.3 kip (326 kN).

Material properties

The material properties used in the analysis, design, and experimental testing of the totally prefabricated counterfort retaining wall system and the soil backfill include the following:

- yield strength of steel reinforcement f_y = 60 ksi (410 MPa)
- steel modulus of elasticity E_s = 29,000 ksi (200,000 MPa)
- concrete compressive strength f_c' = 7.2 ksi (50 MPa)
- unit weight of concrete γ_c = 150 lb/ft^3 (2400 kg/m^3)

Table 1. Concrete compressive strength of different wall components at 28 days

Specimen	Number of specimens	Specimen size, in.	Average ultimate stress, psi
Base	9	6 × 12	9400
Wall	7	6 × 12	7280
Grout	4	3 × 6	7660

Note: 1 in.= 25.4 mm; 1 psi = 6.895 kPa.

- modulus of elasticity of concrete E_c = 4888 ksi (33,700 MPa)
- modular ratio n (E_s/E_c) = 6
- dry unit weight of the soil γ_d = 125 lb/ft^3 (2000 kg/m^3)
- angle of internal friction ϕ_s = 28.0 degrees
- coefficient of active earth pressure k_a = 0.361
- allowable soil bearing capacity assumed for design q_{all} = 2.5 kip/ft^2 (120 kN/m^2) (assumed to obtain worst-case scenario for weak soil conditions)
- allowable soil bearing resistance provided by geotechnical report q_{all_prov} = 10 kip/ft^2 (480 kN/m^2) (actual soil conditions in the field)
- factored soil bearing resistance provided by geotechnical report q_{u_prov} = 15 kip/ft^2 (720 kN/m^2) (actual soil conditions in the field)

Soil properties were obtained from the geotechnical report. For testing purposes, the initial design assumed active earth pressure to mitigate the worst-case scenario. However, the results obtained from the experimental testing and the finite element analysis (as will be discussed in later sections) indicated that the deflection at the top of the wall was too small to initiate minimum active pressure as per Table C3.11.1-1 of the AASHTO LRFD specifications. The final design submitted to the precast concrete facility assumed at-rest soil conditions.

The concrete mixture design proportions include the following:

- sand: 1325 lb/yd^3 (785.2 kg/m^3)
- coarse aggregate: 1527 lb/yd^3 (904.9 kg/m^3)
- cementitious materials: 700 lb/yd^3 (415 kg/m^3)
- water-cement ratio *w/c*: 0.38
- air content: 6.50%

Table 1 shows the results of the concrete average compressive strength properties for each component in the totally prefabricated counterfort retaining wall system. The ultimate compressive strength of concrete was 7200 psi (50 MPa). This value was used for the design and finite element analysis of both the wall and base slab.

Design limit states and stability requirements

Service I and Strength I design limit states are used for load calculations per Table 3.4.1-1 of the AASHTO LRFD specifications. **Table 2** gives the load notation and factors.

The check for stability requirements is performed at the service limit state for the overturning moment, bearing resistance, eccentricity, and sliding. At the strength limit state, stability is checked for bearing resistance, eccen-

Table 2. Load notation and load factors

Load description		Notation	Load Factors		
			Service I	Strength I	
				Minimum	Maximum
Vertical loads	Self-weight of face panel	DC1	1.0	0.9	1.25
	Self-weight of base	DC2			
	Self-weight of counterfort stem	DC3			
	Vertical earth pressure on base heel	EV4	1.0	1.0	1.35
	Vertical earth pressure on base toe	EV5			
	Vertical surcharge load	LSv	1.0	0.0	1.75
Lateral loads	Horizontal earth pressure	PEH	1.0	0.9	1.50
	Horizontal surcharge load	LSh	1.0	0.0	1.75

Table 3. Stability checks based on 2014 AASHTO LRFD specifications 11.6.3

Limit state	Stability check		Factor of safety/limit	Calculated factor of safety	Check
Service I	Failure due to overturning		2	3.39	OK
	Failure due to sliding		1.5	1.55	OK
	Eccentricity limits	1/3 base	5	OK	OK
		2/3 base	10		
	Bearing capacity failure		2.9	2.47	OK
Strength I	Failure due to sliding		1.5	1.8	OK
	Eccentricity limits	1/6 base	2.5	OK	OK
		5/6 base	12.5		
	Bearing capacity failure		7.25	6.41	OK

tricity, and sliding, taking into account the minimum and maximum load combinations specified in sections 11.6.3.2, 11.6.3.3, and 11.6.3.6, respectively, of the AASHTO LRFD specifications. **Table 3** summarizes the stability checks and shows that the design meets the stability requirements per section 11.6.3 of the AASHTO LRFD specifications. The system was not studied for overall stability. The total service load of 144 kip (641 kN) was calculated using a Service I limit state and the total ultimate load of 216.5 kip (963.0 kN) was calculated using a Strength I limit state.

Nonlinear finite element analysis

Simulation software was used to develop a three-dimensional finite element model to analyze the structural behavior of the totally prefabricated counterfort retaining wall system.

Following is the purpose of finite element modeling:

- to verify whether the design based on the AASHTO LRFD specifications satisfies the structural stability and integrity of the system under both service and ultimate loads
- to investigate the deflection of the wall at the top of the wall, *H*/2, and *H*/3, where *H* is the height of wall
- to evaluate the structural behavior of anchors connecting the counterforts and base slab
- to investigate the required amount of steel reinforcement in the counterforts

Concrete, steel reinforcement, and anchors

A three-dimensional solid concrete element model able to simulate both cracking and crushing of concrete was used to simulate the concrete volume. The cracking and crushing of concrete are defined by the Willam and Warnke model, though the crushing capability of concrete was ignored in several studies to avoid fictitious crushing.[28–30] Instead, uniaxial multilinear stress-strain concrete cylinder test data from an actual test specimen were used to define the compressive behavior of concrete. A value of 0.2 was used for the Poisson's ratio of the concrete.

The steel reinforcement and anchors were modeled with the steel link elements. The steel material was assumed to be bilinear elastic-perfectly plastic—that is, identical in both tension and compression—with an elastic modulus of 29,000 ksi (200 GPa) and Poisson's ratio of 0.2.[31] The interface between the concrete elements is assumed to be fully bonded. Contact elements were used to define the frictional interface between the bottom surface of the precast concrete face panel and the top surface of the base slab.

Loading and boundary conditions

A perfectly elastic medium was placed below the retaining wall to mitigate the soil conditions. The finite element

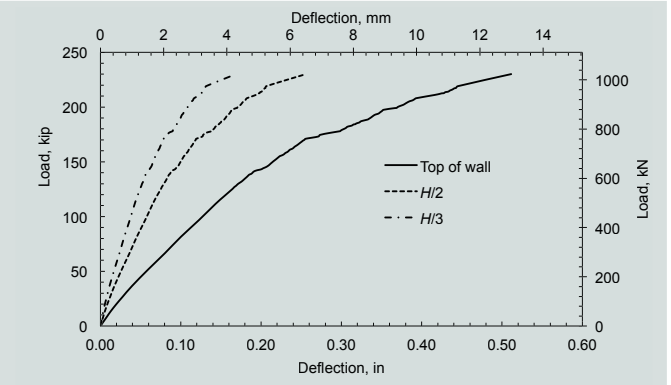

Figure 6. Deflection versus load plots at *H*/3, *H*/2, and top of wall. Note: *H* = height of wall.

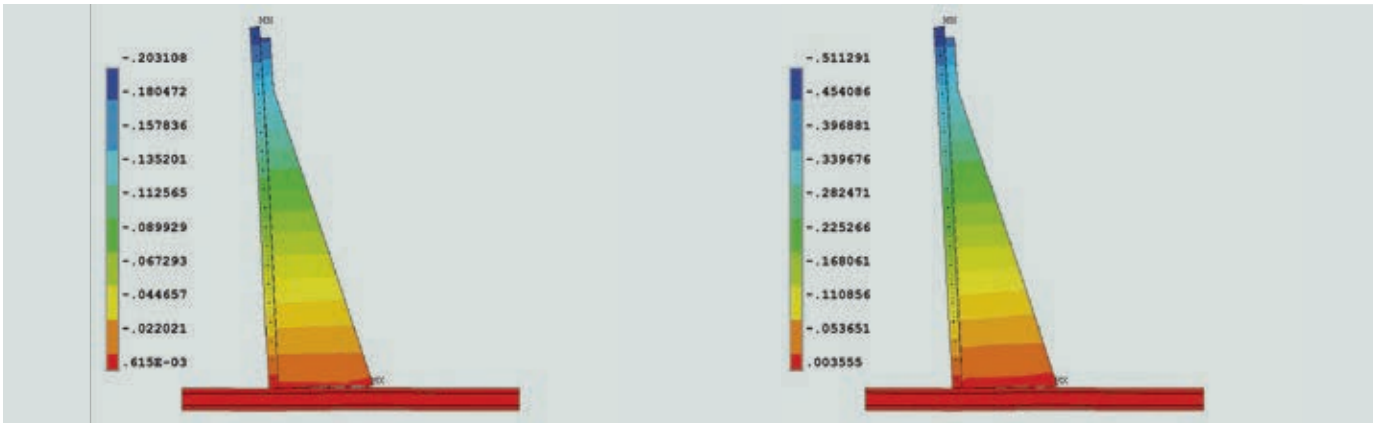

Deflection contours at service load of 144 kip (641 kN)

Deflection contours at ultimate load of 216.5 kip (963.0 kN)

Figure 7. Deflection results obtained from finite element analysis.

model was focused on studying the structural behavior of the totally prefabricated counterfort retaining wall system. Therefore, soil–structure interaction under various soil conditions was ignored. An elastic foundation modulus of 40 ksi (280 MPa) was assigned to the soil medium, which corresponds to medium clay soil. The analysis was conducted over several load steps. The sequence of load steps included the self-weight of the wall, soil backfilling, a 2 ft (0.6 m) surcharge load to simulate the Service I limit state (according to the AASHTO LRFD specifications), and a nodal load of 200 kip (890 kN) from the hydraulic cylinders that was applied at one-third the height of the wall *H*/3 (divided over the three counterforts) to carry the system to ultimate load capacity (Strength I). The nodal load was distributed over a group of nodes that outlines the location on which the actual load was applied during experimental testing.

Analysis and discussion of nonlinear finite element analysis results

The deflections of the wall as well as the variation of the strain in the concrete, steel reinforcement, and anchors are discussed in this section.

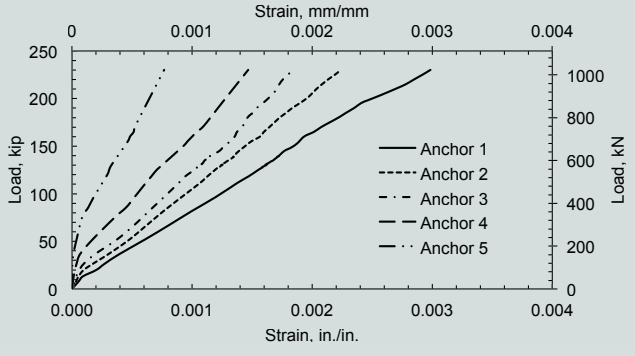

Figure 8. Strain versus applied load at each anchor in the middle counterfort.

Deflection versus load curve **Figures 6** and **7** show the deflection results and deflection contours, respectively, of the totally prefabricated counterfort retaining wall system obtained from finite element analysis at different heights of the face panel. Figure 6 shows that under service loads, the deflection at the top of the wall was estimated to be about 0.21 in. (5.4 mm). In addition, the deflections at midheight *H*/2 and one-third height *H*/3 of the wall were 0.072 and 0.1 in. (1.7 and 2.5 mm), respectively. When the load was increased to 216.5 kip (963.0 kN), the deflection at the top of the wall was 0.44 in. (11 mm) and the deflections at midheight *H*/2 and one-third height *H*/3 of the wall were 0.2 and 0.13 in. (5.2 and 3.3 mm), respectively.

Strain versus stress results in anchors **Figure 8** presents the strain variations in the anchors for the middle counterfort. Figure 8 shows that the strain values exhibit a decreasing general trend starting from the outermost anchor approaching the face of the face panel, as expected. It reveals that anchor 1, the farthest anchor from the face panel (no. 7 [22M] anchor), yielded at a load of 170 kip (760 kN). Anchor 2 shows a yielding strain of 2083×10^{-6} at a load of 215 kip (956 kN). Anchors 3, 4, and 5 did not yield. The described behavior of the anchors was expected because anchors with longer moment arms experience higher flexural moment.

Experimental program

Fabrication

A totally prefabricated counterfort retaining wall system was formed of two totally precast concrete components: the face panel and counterforts, which are cast as one component, and the base slab, which is cast as a separate component. Based on structural analysis supported by finite element analysis, the face panel and counterforts are reinforced with one layer of steel reinforcement. The base slab is reinforced with

two identical layers. **Table 4** summarizes the steel reinforcement of the totally prefabricated counterfort retaining wall system at the level of each component.

Each counterfort is connected to the base slab using five headed anchors. Each headed anchor is embedded 11.5 in. (292 mm) into the base slab. The anchors are placed with 1 ft (0.3 m) spacing starting at 6 in. (150 mm) from the internal face of the wall. The development length of the L bars can also be reduced by reducing the spacing between them. The details for fabrication and erection can be found in Farhat et al.[32]

Instrumentation

Linear variable differential transformers were placed against the face panel of the wall at seven different locations. Four were placed at one-third of the height of the wall and three at midheight of the wall. The purpose of this configuration was to study the deflection of the wall at the counterforts and at the midspan between them. The seven linear variable differential transformers were fixed to a steel frame against the wall and connected to a portable data logger system that provided instantaneous reading of the wall deflection.

Forty-two strain gauges were installed at different locations. Twelve strain gauges were mounted on concrete, and the rest were mounted on steel covering the critical locations of the totally prefabricated counterfort retaining wall system, such as the anchors, the face panel, the base slab, and the main reinforcement in the counterforts and extensions above the counterfort. **Figure 9** shows a typical linear variable differential transformer and strain gauge attachment to the face panel.

For the face panel, strain gauges were used to study the response of the steel at the locations of positive (midspan) and negative (counterfort) moments.

Erection

The erection process is divided into three stages:

1. **Placement of the base slab.** The base slab is placed and leveled on-site. Grout is pumped below the slab to eliminate any voids and to ensure uniform distribution of the soil pressure below the base.

2. **Erection of the wall component.** The wall component is erected using steel cables wrapped in openings in the counterforts intended for handling purposes. The wall is placed and leveled so that each headed anchor is placed in a specified shear pocket.

3. **Grouting of shear pockets.** The shear pockets are grouted to ensure the required anchorage between the base slab from one side and the counterforts from the other side through the headed anchors.

Table 4. Reinforcement details at all wall sections

Assembly part	Number of layers	Vertical	Horizontal	Inclined
Face	One	No. 4 at 12 in.	No. 4 at 12 in.	n/a
Counterfort	One	No. 4 at 12 in.	No. 4 at 6 in.	Four no. 6
Base	Two	No. 5 at 12 in.	No. 5 at 12 in.	n/a
Anchors	n/a	Two no. 7 and three no. 6 on each counterfort		

Note: n/a = not applicable. No. 4 = 13M; no. 5 = 16M; no. 6 = 19M; no. 7 = 22M; 1 in. = 25.4 m.

The erection process was started at the level of the base slab. The base slab was cast and delivered to the site. It was placed 2 ft (0.6 mm) below grade level on spacers, which guaranteed a 1 in. (25 mm) offset from the ground to allow for grouting below the base. The base was grouted to eliminate any voids so that the base would rest uniformly on the ground. The grout was pumped through four holes until all voids below the base were filled. The wall was erected by aligning each headed anchor with the specified shear pocket of the base slab. The shear pockets were then filled with high-performance, fast-setting (15 minutes) grout.

Two circular openings were included in the design of the two external counterforts for handling and erection purposes. The effect of wind load on the stability of the system during construction was calculated and was found to be negligible. Thus, the crane was able to handle the wall without a temporary bracing system.

Setup and testing procedure

Testing on the erected retaining wall was conducted in the following order:

1. **Soil backfilling.** Soil pressure was applied by backfilling the retaining wall with soil with a 95% compaction level.

2. **Surcharge load.** The load was applied using bulldozers to simulate live surcharge conditions.

3. **Test 1.** Two hydraulic cylinders applied up to 178 kip (792 kN) at *H*/3 of the wall acting at six points distributed over three counterforts. It

Instrumentation system showing steel frame with linear variable differential transformers attached

Linear variable differential transformer mounted against face panel

Figure 9. Instrumentation during experimental testing.

Hydraulic pump

North view of setup

Location of load application

Figure 10. Setup for testing the totally prefabricated counterfort retaining wall system in the field.

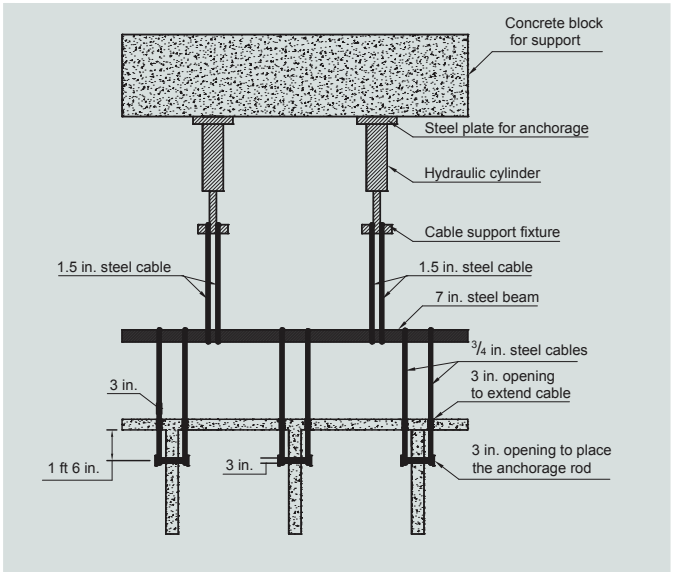

Figure 11. Representation of testing setup as performed in the field. Note: 1 in. = 25.4 mm; 1 ft = 0.305 m.

using a sheep-foot roller compacting machine. The goal was to maintain a 95% compaction level. The proctor test revealed that the wet density of the soil was 130 lb/ft^3 (20 kN/m^3). The moisture level by the end of backfilling was estimated to be 12%. The top surface of the soil was finished at almost a level surface.

Surcharge load To simulate the surcharge load stated by the AAHSTO LRFD specifications that would account for the live load, two vehicular live loads of 27 and 37 kip (120 and 165 kN) were placed at the top of the backfill. A bulldozer was placed 2 ft (0.6 m) away from the wall to simulate a worst-case scenario. The live load application was followed by the application of a lateral load of 16 kip (71 kN) at the top of the wall by a hydraulic cylinder mounted against the bulldozer.

Load application using hydraulic cylinders Tests 1 through 4 were performed using two hydraulic cylinders (**Fig. 10**). The cylinders were anchored to a stack of 10 concrete blocks for additional support. Four 1.5 in. (38 mm) diameter steel cables were hooked to the hydraulic cylinders from one side and to a 7 in. (180 mm) diameter solid steel section from the other side. The solid steel section served as a connection element to transfer the load from the cylinders to the wall. **Figure 11** shows a diagram of the testing setup as performed in the field.

Analysis and discussion of experimental test results

Deflection results

Figures 12 and **13** show the deflection results. The data were collected continuously throughout the project. The testing times are indicated in the figures. After each test was completed, the load was removed. The three linear variable differential transformers located at *H*/2 showed similar readings. The deflections at *H*/2 showed a maximum value of 0.1 in. (2.5 mm) at the end of backfilling. Upon adding the surcharge load, the deflection at *H*/2 increased to 0.115 in. (2.85 mm). Finally, the registered deflection at tests 1, 2, 3, and 4 were 0.158, 0.160, 0.163, and 0.212 in. (4.01, 4.06, 4.14, and 5.38 mm), respectively.

The deflection results show that the critical locations at left midspan, middle counterfort, and right midspan at *H*/3 of the wall exhibit a similar behavior. Figure 13 shows that the maximum deflection at *H*/3, recorded during test 4, was found to be 0.167 in. (4.25 mm) at the left counterfort. A slightly smaller value of 0.14 in. (3.6 mm) was recorded by the three other linear variable differential transformers at the same level.

The test results show consistent deflection values between the counterforts and the midspans of the walls throughout various testing times. This is due to the efficient geometric configuration that minimizes the load resisted by the face panel. The counterforts are designed to resist the total lateral load, while the face panel is designed to resist the lateral load due to soil pressure in the longitudinal direction spanning two counterforts. Thus, using a small

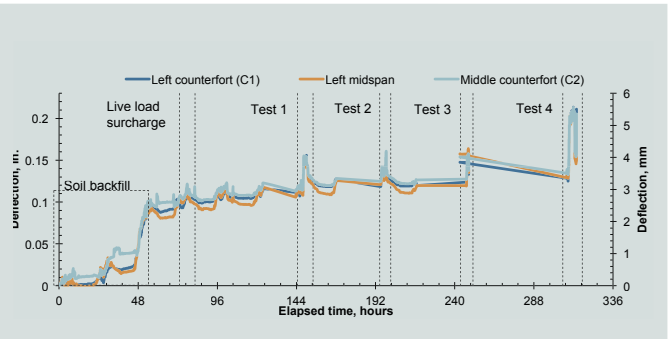

Figure 12. Deflection measured by the three linear variable differential transformers at *H*/2. Note: *H* = height of wall.

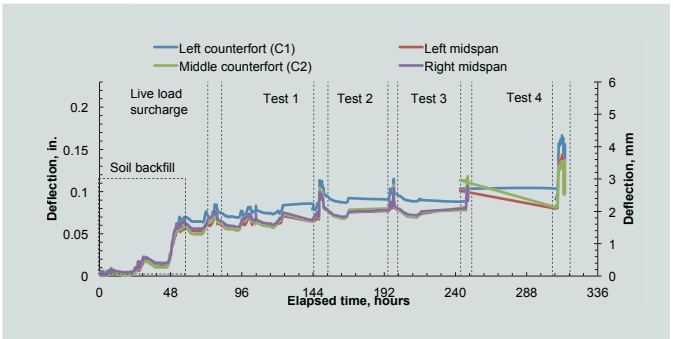

Figure 13. Deflection measured by the four linear variable differential transformers at *H*/3. Note: *H* = height of wall.

spacing-to-height ratio (0.245) minimizes the lateral loads caused by soil pressure on the face panel.

To assume active earth pressure, the AASHTO LRFD specifications specify a deflection-to-height ratio ranging from 0.001 to 0.01 for soil types varying from dense sand to compacted clay, respectively ($0.001 < D/H < 0.01$, where D is the deflection at the top of the wall). The value of deflection necessary to initiate active earth conditions corresponding to a wall height of 20 ft 2 in. (6.09 m) varies from 0.241 to 2.41 in. (6.12 to 61.2 mm). The maximum deflection obtained from the experimental testing at service limit state was about 0.212 in. (5.39 mm). This indicates that the deflection at the top of the wall was too small to initiate the minimum active pressure per Table C3.11.1-1 of the AASHTO LRFD specifications. Thus, the design of the counterfort retaining wall in future applications should consider at-rest earth conditions.

Strain in the anchors

Figure 14 presents the maximum strain readings in the headed anchors at the middle and left counterforts. Figure 20 shows that the strain results in the headed anchors varied depending on the location of the anchor with respect to the wall and location of the counterfort. The outermost two anchors from the face panel gave the highest strain readings due to their longer moment arms with respect to the wall. These readings gradually decreased in the anchors closer to the wall. The strain readings in anchors 1 and 2 at the middle counterforts were 2659×10^{-6} and 2203×10^{-6}, respectively, and therefore exceeded the yield limit strain of steel, 2070×10^{-6}. The strain reading in anchor 1 at the left counterfort was found to be 2421×10^{-6}, which also exceeded 2070×10^{-6}. However, anchor 2 showed a strain value of 2010×10^{-6}, which is close to the yield limit strain of steel.

Figure 15 shows the strain variation at the testing times for anchor 1 (no. 7 [22M] bar), located at the left counterfort throughout various loading conditions. During soil backfilling, the strain increased to 1360×10^{-6}. It was then followed by a gradual increase throughout testing. This increase was in the form of sharp spikes whenever the load was applied by hydraulic cylinders. The spikes were followed by drops as soon as the load was removed. This indicates that the anchors did not yield until loaded to an ultimate load (test 4). The yielding limit of the anchor was observed in test 4, where it reached 2421×10^{-6} when subjected to an ultimate load of 192.4 kip (855.8 kN).

The high tensile strain result in the outermost anchors is expected because of the large moment arm measured from the outside face of the face panel to the center of each anchor. As a result, the design is controlled by the outermost anchors, for which no. 7 (22M) bars or higher are recommended. Smaller bar sizes can be used for anchors close to the face panel (anchors 4 and 5) because they experience smaller tensile strain. The anchors also play an important role in maintaining the overall stability of the system.

Figure 15 also shows a pattern in the strain readings of gradual increases followed by decreases over time between tests. A gradual drop in the strain reading was observed during nighttime and the inverse during the day. This is attributed to temperature variations between day and night as the test was performed in field conditions.

Face panel and main reinforcement in the counterfort

A thorough visual inspection of the face panel revealed no visible cracks in the front of the face panel during testing. This is attributed to the efficiency of the geometric configuration, which helped lower the stresses in the face panel and achieved a successful design using one layer of steel with a wall thickness of 6 in. (150 mm). The results showed that no yielding occurred in the main reinforcement of the face panel. **Figure 16** shows sample strain readings in the face panel at the left midspan between counterforts and over the middle counterfort. The maximum strain readings at $H/3$ at the midspan between the counterforts and over the counterforts were similar and ranged from 500 to 600×10^{-6}.

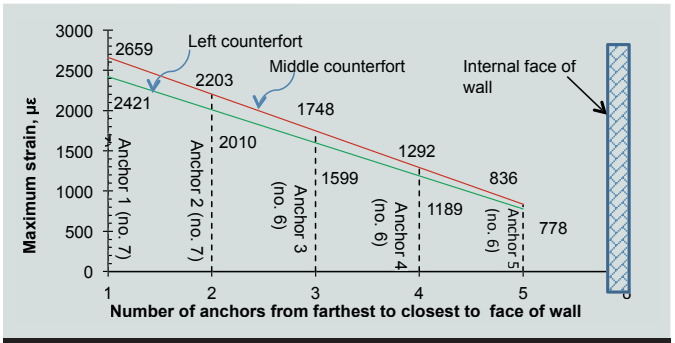

Figure 14. Maximum strains in headed anchors at the middle and left counterforts. Note: Strain units are microstrain.

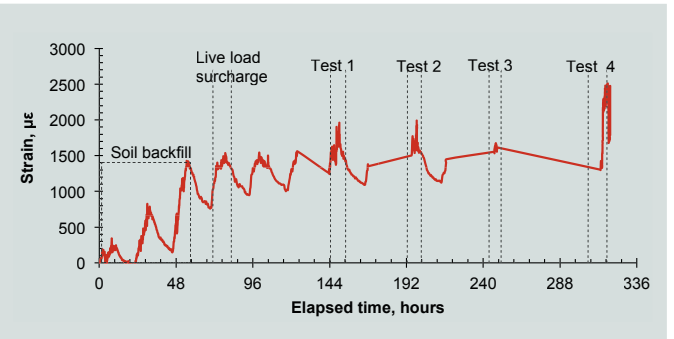

Figure 15. Strain variation curve at the times of testing for anchor 1 in left counterfort. Note: Strain units are microstrain.

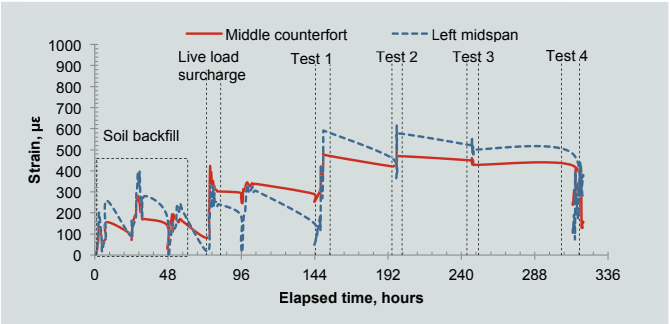

Figure 16. Time versus strain readings for face panel steel reinforcement located at *H*/3 at the middle counterfort and left midspan. Note: Strain units are microstrain. *H* = height of wall.

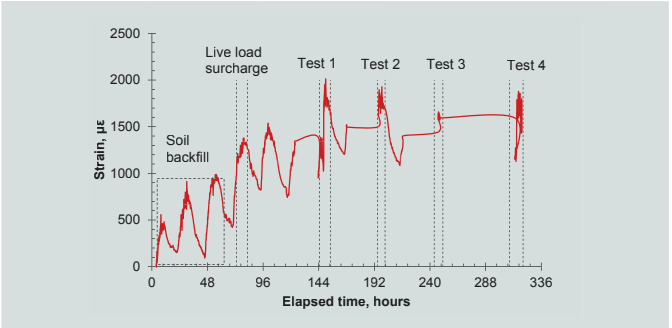

Figure 17. Strain readings at the main reinforcement of the right and middle counterforts. Note: Strain units are microstrain.

Figure 17 gives the strain readings at the main reinforcement of the right and middle counterforts. The strain readings show a maximum value of 1957.5 × 10^{-6} recorded in test 1 and almost similar values recorded in tests 2 and 4. These values dropped to their initial values after each test. This indicates that the main reinforcement did not undergo yielding. This behavior was not witnessed in test 3 due to the nature of the loading setup, which only focused on the behavior of the middle counterfort.

Cracks developed in the concrete at the level of the inclined surface to the counterforts due to a high overturning moment resisted by the T section of the counterforts and the face panel. This observation was verified using finite element analysis (**Fig. 18**).

The finite element analysis revealed an important aspect of the counterfort behavior. Anchors are subjected to tension when the lateral loads are applied. Thus, cracks are expected to generate at the location of the anchors. These cracks are likely to propagate toward the middle of the counterfort as the load increases, as proved by the finite element analysis. (Fig. 24).

In this case, shear failure will be the dominant mode of failure due to the large counterfort depth. Temperature and shrinkage reinforcement (vertical bars) are used to control the mode of failure by arresting the cracks propagating toward the middle of the counterfort web. Thus, the failure mode of the counterforts can be controlled by reducing the spacing of the vertical bars to obtain a controlled flexural mode of failure.

Results and analysis for strain in top extension steel

Figure 19 shows the strain readings in the steel at the top extension of the left and middle counterforts. It shows that the strain readings of the steel reinforcement at the top of the counterforts at the extension steel exhibited no significant changes except in test 1. In test 1, a 16 kip (71 kN) load was applied at the top of the wall using a hydraulic cylinder mounted against the bulldozer, which in turn was used as live load surcharge resulting in high bending stresses at the level of the extension steel. These stresses were reflected in a high jump in the strain readings: 1100 × 10^{-6} in the left counterfort and about 1700 × 10^{-6} in the middle counterforts. These strain readings indicate that the steel at the top of the counterforts did not yield when subjected to a lateral load of 16 kip.

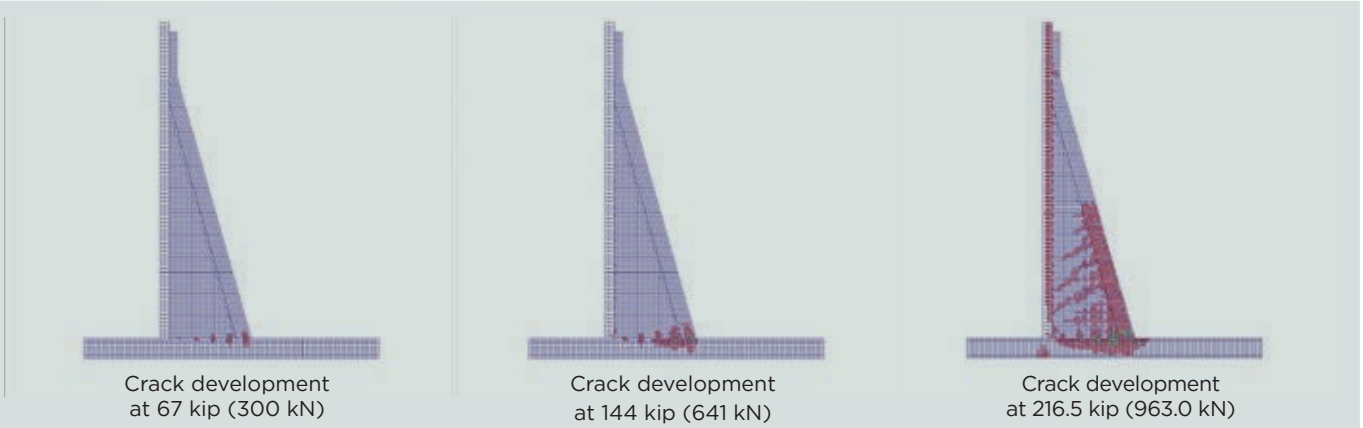

Figure 18. Development of cracks in the counterforts and base slab using finite element analysis.

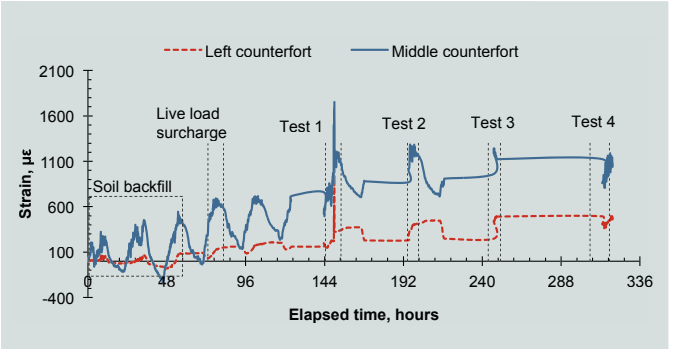

Figure 19. Strain readings in steel at the top extension of the left and middle counterforts. Note: Strain units are microstrain.

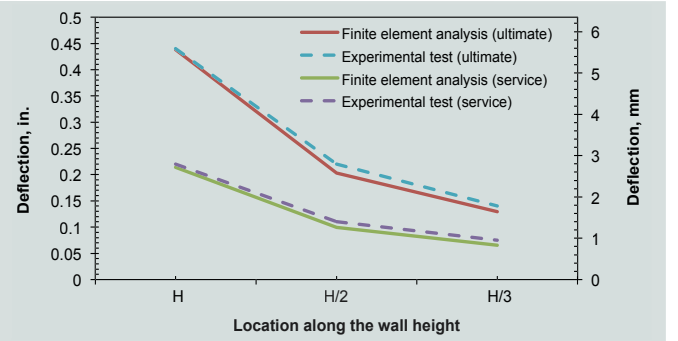

Figure 20. Deflection results from the experimental test and nonlinear finite element analysis at service load.

Validation of nonlinear finite element analysis results with experimental results

At service load, the finite element analysis deflection results at *H*/2 and *H*/3 of the wall were 0.1 and 0.065 in. (2.5 and 1.6 mm), respectively. The experimental results showed average deflections at *H*/2 and *H*/3 equal to 0.11 and 0.075 in. (2.8 and 1.9 mm), respectively. In addition, the nonlinear finite element analysis deflections at ultimate load at *H*/2 and *H*/3 were 0.203 and 0.13 in. (5.16 and 3.3 mm), respectively. The experimental results at ultimate load showed average deflections at *H*/2 and *H*/3 of 0.22 and 0.14 in. (5.6 and 3.5 mm), respectively. The nonlinear finite element analysis results are in good agreement with the experimental results (**Fig. 20**).

The deflection at the top of the wall was estimated using linear extrapolation for the experimental results. The deflection values at the top were found to be 0.22 in. (5.6 mm) at service load and 0.44 in. (11 mm) at ultimate load. The results obtained from linear extrapolation were confirmed using nonlinear finite element analysis. **Table 5** summarizes the experimental test results compared with the nonlinear finite element analysis results.

The finite element analysis results for the headed anchors showed a good correlation with the experimental test results. The finite element analysis showed that at ultimate load, the strain was estimated to be about 2780×10^{-6} in the outermost anchor at 215.5 kip (963.0 kN) load (test 4). In addition, the trend obtained from the finite element analysis at ultimate load showed that yielding occurs at the first two anchors (anchors 1 and 2). The strain readings in the anchors decreased as they were taken closer to the face panel (moving from anchor 1 to 5).

Figure 21 presents a comparison of strain readings in the anchors between the experimental test results and the finite element analysis results. It shows that the results obtained from the finite element analysis are validated by those obtained from the experimental testing. The anchors exhibited a trend consistent with that of the experimental results. The finite element model verified the behavior exhibited by the totally prefabricated counterfort retaining wall system during experimental testing.

Conclusion

Full-scale experimental testing and nonlinear finite element analysis were performed to examine the overall structural behavior of a totally prefabricated counterfort retaining wall system. The wall was 20 ft 2 in. (6.09 m) high and 13 ft 10 in. (4.21 m) wide. The system was optimized using conventional beam theory and finite element analysis.

Headed anchors played the most important role in enforcing full composite action between the counterfort and the base slab. The wall was subjected to soil backfilling, live load surcharge, and additional loads of up to 192.4 kip (855.8 kN) using hydraulic cylinders to bring the system to ultimate load. The deflection in the face panel at *H*/3 and *H*/2 was monitored. In addition, strain readings in the headed anchors, main counterfort reinforcement, face panel, and base slab were monitored.

Based on the experimental test and the finite element analysis results, the following can be concluded:

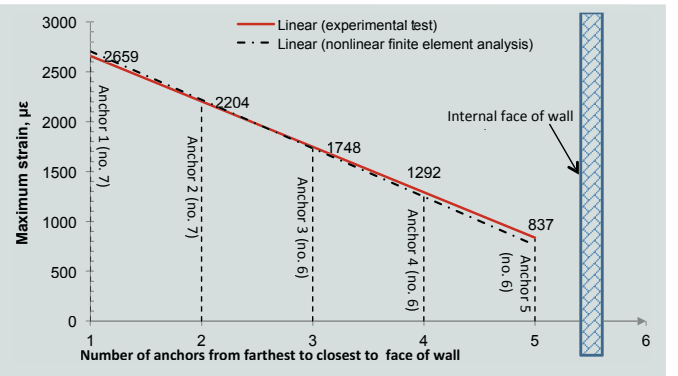

Figure 21. Comparison of strain readings in the anchors between experimental results and nonlinear finite element analysis. Note: Strain units are microstrain. no. 6 = 19M; no. 7 = 22M.

Table 5. Summary of deflection results compared with nonlinear finite element analysis

Load level	Location	Experimental data, in.	Nonlinear finite element analysis data, in.	Difference, %
Ultimate load (216 kip)	*H*	0.440	0.438	0.40
	H/2	0.220	0.203	7.59
	H/3	0.140	0.129	7.57
Service load (144 kip)	*H*	0.220	0.214	2.82
	H/2	0.110	0.099	9.62
	H/3	0.075	0.065	12.74

Note: *H* = height of wall. 1 in. = 25.4 mm; 1 kip = 4.448 kN.

- Headed anchors showed excellent performance in maintaining the composite action between the precast concrete wall and the base slab at service and ultimate loads. This was verified by the nonlinear finite element analysis and the experimental testing. The deflection measured at the midheight of the wall was found to be about 0.2 in. (5 mm). Counterforts added stiffness to the structure by increasing the section at which the bending moment is resisted due to the applied load. The L bars that connected the face panel to the stems were found to be effective in maintaining the composite action between both components.

- The strain readings in the anchors indicate that the outermost anchors experienced the highest strain. The design is controlled by the outermost anchors, and smaller bar sizes can be used for anchors close to the face panel because they experience smaller tensile strain. In addition, the strain readings in the main steel of the counterforts showed that the counterforts resist the entire subsequently applied load. Therefore, the following two assumptions can be made by the designer:

  — The anchors should be properly designed to resist the entire applied bending moment and shear forces.

  — When the anchors are designed, the main steel in the counterforts should be designed to resist the entire lateral load, assuming that the bottom of the counterforts is fully bonded to the base slab. The anchors also play an important role in maintaining the overall stability of the system.

- The steel in the face panel showed insignificant and almost equivalent readings in the positive and negative regions. This supports the assumption that the cross section can be significantly reduced and one layer of steel can be used to resist both positive and negative bending moments. This reduces the overall volume of concrete, which provides great advantages in transportation and cost reduction.

- Cracks can initiate in the regions of the internal anchors that are subjected to tensile stresses. These cracks propagate toward the web of the counterforts as the load increases. The spacing between the vertical reinforcement in the counterfort stems should be reduced to 6 in. (150 mm) to provide an arrest mechanism for the cracks and prevent shear failure in the counterforts, as verified by finite element analysis.

- The totally prefabricated counterfort retaining wall system exhibited a sufficiently good performance for use in highway applications. It satisfies the need for fast-track construction. Although the impact factor specified by the AASHTO LRFD specifications was implemented in the design, further research might be required to study the behavior of totally prefabricated counterfort retaining wall systems under traffic collision force.

Acknowledgments

This study was funded and supported by Utility Concrete Products LLC (UCP) in Morris, Ill. The authors thank UCP for performing the fabrication and erection and for providing all of the means for the experimental testing that was performed at the UCP facility. In addition, the authors thank Claudio Fazio from V3 for his help and support. Special thanks go to all who provided help and support to complete this project.

References

1. Farhat, M., M. Rahman, M. Ibrahim, and M. A. Issa. "Design Optimization and Modeling of a Totally Precast Concrete Counterfort Retaining Wall System"

In *16th European Bridge Conference in Edinburgh, UK, 22–25 June 2015*. Edinburgh, UK: ECS Publications.

2. Farhat, M., M. Rahman, M. Ibrahim, and M. A. Issa. 2014. "Design, Fabrication, Modeling and Experimental Study of a Totally Precast Concrete Counterfort Retaining Wall System for Highways." In *60th Anniversary 2014 Convention and National Bridge Conference Proceedings*. Chicago, IL: PCI. CD-ROM.

3. Senthil, K., M. A. Iqbal, and A. Kumar. 2014. "Behavior of Cantilever and Counterfort Retaining Walls Subjected to Lateral Earth Pressure." *International Journal of Geotechnical Engineering* 8 (2): 167–181.

4. AASHTO (American Association of State Highway and Transportation Officials). 2014. *AASHTO LRFD Bridge Design Specifications*. 7th ed., customary U.S. units. Washington, DC: AASHTO.

5. Biswas, M. 1986. "Precast Bridge Deck Design Systems." *PCI Journal* 31 (2): 40–94.

6. Hieber, D. G., J. M. Wacker, M. O. Eberhard, and J. F. Stanton. 2005. *State-of-the-Art Report on Precast Concrete Systems for Rapid Construction of Bridges*. Report WA-RD 594.1. Olympia, WA: Washington State Department of Transportation.

7. Goldberg, D. 1987. "Precast Prestressed Concrete Bridge Deck Panels." *PCI Journal* 32 (2): 26–45.

8. PCI Northeast Technical Committee. 2001. *Precast Deck Panel Guidelines*. Report PCINER-01-PDPG. Belmont: MA: PCI Northeast.

9. PCI Northeast Technical Committee. 2002. *Full Depth Precast Concrete Deck Slabs*. Report PCINER-02-FD-PCDS. Belmont: MA: PCI Northeast.

10. Tadros, M. K., and M. C. Baishya. 1998. *Rapid Replacement of Bridge Decks*. NCHRP (National Cooperative Highway Research Program) report 407. Washington, DC: NCHRP.

11. Issa, M. A., A. A. Yousif, and M. A. Issa. 1995. "Construction Procedures for Rapid Replacement of Bridge Decks." *Concrete International* 17 (2): 49–52.

12. Issa, M. A., A. A. Yousif, M. A. Issa, I. I. Kaspar, and S. Y. Khayyat. 1995. "Field Performance of Full Depth Precast Concrete Panels in Bridge Deck Reconstruction." *PCI Journal* 40 (3): 82–108.

13. Issa, M. A., A. A. Yousif, and M. A. Issa. 2000. "Experimental Behavior of Full-Depth Precast Concrete Panels for Bridge Rehabilitation." *ACI Structural Journal* 97 (3): 397–407.

14. Issa, M. A., A. Idriss, I. I. Kaspar, and S. Y. Khayyat. 1995. "Full Depth Precast and Precast, Prestressed Concrete Bridge Deck Panels." *PCI Journal* 40 (1): 59–80.

15. Issa, M. A., A. A. Yousif, M. A. Issa, I. I. Kaspar, and S. Y. Khayyat. 1998. "Analysis of Full Depth Concrete Bridge Deck Panels." *PCI Journal* 43 (1): 74–85.

16. Billington, S. L., R. W. Barnes, and J. E. Breen. 2001. "Alternate Substructure Systems for Standard Highway Bridges." *Journal of Bridge Engineering* 6 (2): 87–94.

17. Billington, S. L., R. W. Barnes, and J. E. Breen. 1998. *A Precast Substructure Design for Standard Bridge Systems*. Report 1410-2F. Austin, TX: Center for Transportation Research, University of Texas at Austin.

18. Culmo, M. P. 1991. "Bridge Deck Rehabilitation Using Precast Concrete Slabs." In *Eighth Annual International Bridge Conference Proceedings, June 1991, Pittsburgh, Pennsylvania*, IBC-91-55, 389–396. Pittsburgh, PA: Engineers' Society of Western Pennsylvania.

19. Culmo, M. P. 2000. "Rapid Bridge Deck Replacement with Full-Depth Precast Concrete Slabs." *Transportation Research Record* 1712: 139–146.

20. Badie, S. S., M. C. Baishya, and M. K. Tadros. 1998. "NUDECK—An Efficient and Economical Precast Prestressed Bridge Deck System." *PCI Journal* 43 (5): 56–74.

21. LoBuono, Armstrong, and Associates. 1996. "Development of Precast Bridge Structures." Report prepared for the Florida Department of Transportation.

22. Medlock, R., M. Hyzak, and L. Wolf. 2002. "Innovative Prefabrication in Texas Bridges." In *Proceedings of the Texas Section, American Society of Civil Engineers, Spring Meeting, March 2002*. Austin, TX: American Society of Civil Engineers—Texas Section.

23. Hewes, J. T. 2013. *Analysis of the State of the Art of Precast Concrete Bridge Substructure Systems*. Report FHWA-AZ-13-687. Phoenix, AZ: Arizona Department of Transportation Research Center.

24. Darwish, I., and M. Kasi. 2013. "Innovative Precast Concrete Cantilever Retaining Wall System." *Aspire*, Spring, 21.

25. Stamnas, P. E., and M. D. Whittemore. 2005. "All-Precast Substructure Accelerates Construction of Prestressed Concrete Bridge in New Hampshire." *PCI Journal* 50 (3): 26–39.

26. Donkada, S., and D. Menon. 2012. "Optimal Design of Reinforced Concrete Retaining Walls." *The Indian Concrete Journal*, April: 9–18.

27. Culmo, M. P. 2009. *Connection Details for Prefabricated Bridge Elements and Systems*. FHWA-IF-09-010. McLean, VA: Federal Highway Administration, U.S. Department of Transportation.

28. Kachlakev, D., T. Miller, S. Yim, K. Chansawat, and T. Potisuk. 2001. *Finite Element Modeling of Concrete Structures Strengthened with FRP Laminates*. SPR 316. Salem, OR: Oregon Department of Transportation.

29. Zhou, S., D. C. Rizos, and M. F. Petrou. 2004. "Effects of Superstructure Flexibility on Strength of Reinforced Concrete Bridge Decks." *Computers & Structures* 82 (1): 13–23.

30. Si, B. J., Z. G. Sun, Q. H. Ai, D. S. Wang, and Q. X. Wang. 2008. "Experiments and Simulation of Flexural-Shear Dominated RC Bridge Piers under Reversed Cyclic Loading." In *The 14th World Conference on Earthquake Engineering Proceedings, October 2008, Beijing, China*. Heilongjiang, China: Chinese Association of Earthquake Engineering.

31. Al-Rousan, R., and M. Issa. 2011. "Fatigue Performance of Reinforced Concrete Beams Strengthened with CFRP Sheets." *Construction and Building Materials* 25 (8): 3520–3529.

32. Farhat, M., and Issa, M. A. "Fabrication and Construction of Totally Prefabricated Counterfort Retaining Wall System for Highways." *Practice Periodical on Structural Design and Construction* 22 (2). Published electronically .

Notation

D = deflection at top of the wall

E_c = modulus of elasticity of concrete

E_s = steel modulus of elasticity

f'_c = concrete compressive strength

f_y = yield strength of steel reinforcement

H = height of wall

k_a = coefficient of active earth pressure (AASHTO LRFD specifications 3.11.5.7.1)

L = center-to-center spacing between two adjacent counterforts

n = modular ratio E_s/E_c (AASHTO LRFD specifications 5.7.1)

q_{all} = allowable soil bearing capacity assumed for design

q_{all_prov} = allowable soil bearing resistance provided by geotechnical report

q_{u_prov} = factored soil bearing resistance provided by geotechnical report

w/c = water-cement ratio

ϕ_s = angle of internal friction

γ_c = unit weight of concrete

γ_d = dry unit weight of soil

About the authors

Maen Farhat is a graduate research assistant and PhD candidate in the department of Civil and Materials Engineering at the University of Illinois at Chicago. His current research interests are accelerated bridge construction, precast concrete, and recycled high-density polyethylene crossties for high-speed rail applications.

Mustapha Ibrahim is a graduate research assistant and PhD candidate in the department of Civil and Materials Engineering at the University of Illinois at Chicago. He is involved in various research topics including concrete materials with an emphasis on concrete durability and sustainability, applications of advanced composites in concrete, and ultra-high-performance concrete.

Mohsen Issa, PhD, PE, SE, FACI, FASCE, is a professor of structural and materials engineering in the department of Civil and Materials Engineering at the University of Illinois at Chicago. His research interests include structural buildings and bridges, development of experimental and analytical techniques for monitoring and rating existing highway bridges, advanced composites, concrete durability, recycled plastic materials, accelerated bridge construction techniques, and sustainability.

Momenur Rahman is a graduate research assistant in the department of Civil and Materials Engineering at the University of Illinois at Chicago. He is involved in various research topics including finite element analysis, behavior of beam-column joints under seismic loading, lightweight concrete, and applications of advanced composites in concrete.

Abstract

The overall structural behavior of a totally prefabricated counterfort retaining wall system was examined experimentally and analytically using nonlinear finite element analysis. A 20 ft 2 in. (6.09 m) high, 13 ft 10 in. (4.21 m) wide full-scale prototype was designed meeting the requirements of the AASHTO LRFD specifications, assembled, constructed, instrumented, and tested in a precast concrete plant. The design was optimized and validated using nonlinear finite element analysis. Five headed anchors extended from each counterfort and were grouted to the base slab using truncated conical shear pockets to ensure full connectivity between the precast concrete components.

The results obtained from the experimental testing show that the wall experienced a deflection of 0.2 in. (5 mm) at its middle. Moreover, the anchors succeeded in maintaining serviceability and ultimate strength requirements. The totally prefabricated precast concrete counterfort retaining wall system has proven to be an innovative and effective solution for multiple requirements such as speed of construction, strength, durability, and safety.

Keywords

Accelerated construction, assessment and monitoring, construction, creative/innovative solutions and structures, headedanchors, retaining wall.

Review policy

This paper was reviewed in accordance with the Precast/Prestressed Concrete Institute's peer-review process.

Reader comments

Please address reader comments to journal@pci.org or Precast/Prestressed Concrete Institute, c/o *PCI Journal*, 200 W. Adams St., Suite 2100, Chicago, IL 60606.